An Iterative Procedure for Nonlinear Flutter Analysis

Craig L. Lee*

Texas Instruments Incorporated, Lewisville, Texas

An iterative procedure in the frequency domain is presented for flutter analysis of large dynamic systems with multiple structural nonlinearities. The major components of the procedure are the describing function approach for system linearization, a structural dynamics modification method for shifting system mode shapes and frequencies, and a complex eigenvalue algorithm for solution of the flutter equation. The purpose of the procedure is to achieve alignment of the oscillatory amplitude in each nonlinear spring with the describing function prediction of stiffness before computing the final stability characteristics. The result is a system tuned to the flutter frequency at the time of instability. To support the development and validation of the procedure, several describing functions are formulated and a quantitative measure of the errors in each is presented. Validation of the iterative method is accomplished through examples involving dynamic systems of increasing complexity, coupled with various representations of the unsteady aerodynamic forces. Both numerical simulations and experimental data are used to compare with the iterative predictions. In the cases studied, the agreement is good to excellent, with the method accurately predicting the amplitude of a limit cycle flutter as well as the initial disturbance required to produce flutter.

Introduction

F LUTTER predictions for nonlinear dynamic systems have been hindered in the past by limitations in the analytical methods. Contemporary flutter techniques capable of handling multiple degree-of-freedom (dof) systems coupled with advanced unsteady aerodynamics consider them to be linearly elastic, while those that deal with the nonlinear systems impose severe restrictions on the number of nonlinearities, the size of the system, or the aerodynamic formulation. As the number or magnitude of structural nonlinearities in a given system becomes significant, the assumption of linear elasticity results in a poor estimation of the stability boundary. Since virtually all tactical missile systems as well as aircraft structures contain some concentrated nonlinearities, their prominence in the analysis of wing and control surface flutter is increasing.

Relevant studies into the effects of nonlinearities on the flutter characteristics of wings and control surfaces can be found in Refs. 1-12. These studies have shown that nonlinearities influence not only the flutter speed, but also the characteristics of the flutter motion. In contrast to the linear system with its exponential growth in amplitude at the time of instability, the nonlinear system can achieve a state of equilibrium between elastic, inertial, and aerodynamic forces that is ultimately manifested as a stable limit cycle oscillation. Also, the stability of the nonlinear system may become functionally dependent on the amplitude of the initial disturbance. The magnitude of this disturbance, contrary to linear system behavior, can result in a number of stability states ranging from stable to a condition of divergent flutter.

Analytical techniques that deal directly with structural nonlinearities in the aeroelastic stability problem can be grouped largely into two categories: 1) analog simulation or numerical integration of the nonlinear differential equations of motion in the time domain and 2) linearization of the nonlinear system through application of the describing function[16] approach or method of "harmonic balance" in the frequency domain. The earliest studies into the nonlinear

flutter phenomena were primarily analog in nature and concentrated on establishing an understanding of the mechanism rather than developing extensive analytical procedures. Woolston et al.,[1,2] Shen,[3] and Breitbach[4,5] conducted their initial investigations on simple dynamic systems that could be easily represented mathematically. The computation of the unsteady aerodynamic forces was typically accomplished through application of Theodorsen's[13] equations for two-dimensional incompressible flow. This approach was advantageous because the formulation could readily be expressed in either the reduced frequency domain or the time domain using Wagner's[14] or Küssner's[15] function for arbitrary motion. The relatively simple aerodynamics coupled with a 2 or 3 dof dynamic system presented a very manageable set of differential equations and achieved the intended goal of focusing attention on the effects of the nonlinearities. Today, with the complexity of missile control surface design increasing, application of more advanced three-dimensional aerodynamic techniques such as the Mach box method[17] or the doublet lattice method[18] is needed to produce the most efficient designs. However, these approaches were developed in the frequency domain for use with the normal mode formulation of the equations of motion and a transformation to the time domain for arbitrary motion is cumbersome and inefficient. Thus, the development of techniques for nonlinear flutter analysis that use these methods cannot easily rely on time domain simulations to produce "experimental" data for verification. In the absence of wind tunnel or flight data, the alternative is to implement the simpler formulations and assume that validation based on them is extendable to the more advanced aerodynamic methods. This approach has been taken in the present study in conjunction with a limited amount of flight data.

Aside from Laurenson and Trn's[7] solution for a system with two interacting nonlinearities, Breitbach's[6] work in 1980 was the first published that dealt with the problem of multiple nonlinearities in large dynamic systems. He proposed an iterative procedure in the frequency domain that recognized the need to align the oscillatory amplitude in each nonlinear spring with the describing function prediction of stiffness before a consistent set of solutions could be obtained. The present study, in addition to recognizing this need, uses an iterative procedure in which the system mode shapes and frequencies are shifted during the alignment process. This produces a system tuned to the flutter frequency at

the time of instability. Conducting the procedure over a range of amplitudes at a preselected reference degree of freedom then allows complete stability boundaries to be constructed.

The Iterative Procedure

Use of the describing function method for characterizing concentrated structural nonlinearities results in a linearized approximation to the nonlinear system. The method yields a functional relationship between the stiffness of the nonlinear spring and its displacement during the application of a dynamic load. Producing a linearized system allows the use of conventional flutter methods such as the normal mode approach. In turn, this has the distinct advantage of representing a large dynamic system as a computationally manageable truncated series of normal modes. Several problems arise, however, when applying the describing function method to large systems with multiple nonlinearities. A dynamic system excited by an external oscillatory forcing function of prescribed amplitude and frequency will produce a unique displacement in each of the nonlinear springs. These displacements correspond to a single set of stiffness values per the appropriate describing functions. Calculation of the nonlinear spring displacements is usually accomplished through normal mode summation or the mode-superposition method. However, this approach requires prior knowledge of the normal mode shapes of the system, which are themselves a function of the stiffness values of each nonlinear spring. From a rigorous analytical standpoint then, it becomes necessary to align the nonlinear spring displacements produced by the external forces with the stiffness terms used to compute the system mode shapes. The aeroelastic stability problem is further complicated by the dependence of the unsteady aerodynamic forces on these mode shapes. Nevertheless,the amplitude-stiffness alignments can be accomplished by an iterative procedure in the frequency domain.

Figure 1 illustrates movement through the procedure, beginning with the determination of natural frequencies and mode shapes of the dynamic system with some nominal values of stiffness for the nonlinear springs. After calculation of the generalized aerodynamic forces using aerodynamic influence coefficients, the normal mode flutter equation is solved, yielding n complex eigenvalues and eigenvectors. Because each of the n flutter solutions is associated with a distinct oscillatory frequency, each will produce a unique set of displacements in the nonlinear springs. Consequently, only one of these unique sets is selected for alignment with the nonlinear spring stiffnesses (i.e., the one suspected of being unstable). This is equivalent to considering the unsteady aerodynamics as a family of forcing functions, each at a distinct frequency, and tracking the effect of each throughout the flutter analysis. This approach is considered valid because, at the time of instability, the response of the system is sharply peaked only at the flutter frequency as noted by Shen.[3] Under these conditions, the alignment procedure produces a dynamic system that is tuned to that specific flutter frequency.

With the μth eigenvalue of interest selected, the procedure continues with the calculation of displacements in each nonlinear spring. Normal mode summation is employed along with an assumed displacement at one of the system's degrees of freedom, usually a translation or rotation of a structural node point on the control surface. This reference displacement, d_R, represents the amplitude of a limit cycle oscillation or the magnitude of the initial disturbance for which the system stability characteristics are being investigated. An initial scale factor, $\alpha_R^{(0)}$, is computed at the reference dof as

$$d_R = \alpha_R^{(0)} [\Phi_R]^{(0)} \{\Psi_\mu\}^{(0)} \qquad (1)$$
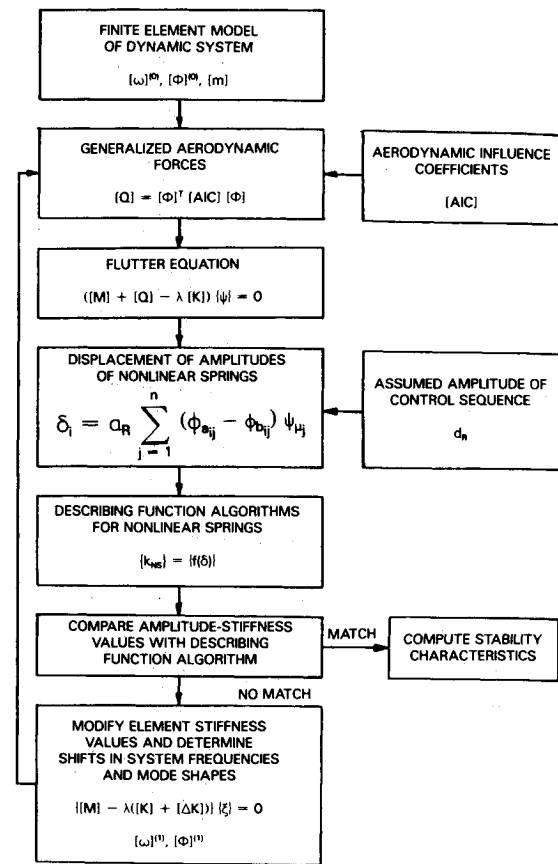

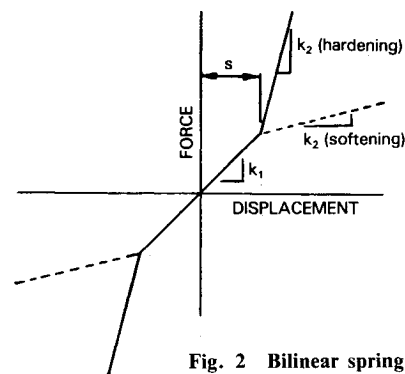Fig. 1 Flow chart of iterative procedure.

Fig. 2 Bilinear spring.

where $[\Phi_R]$ is the row matrix of eigenvector terms for the reference dof and $\{\Psi_\mu\}$ the preselected μth column of modal amplitudes from the flutter solution. The net displacement of the ith nonlinear spring is then given by

$$\delta_i^{(0)} = \alpha_R^{(0)} \sum_{j=1}^{n} (\phi_{a_{ij}}^{(0)} - \phi_b^{(0)})\Psi_{\mu_j}^{(0)} \qquad (2)$$

where a and b designate the two dof associated with the nonlinear spring. The complete set of nonlinear spring displacements is

$$\{\Delta\}^{(0)} = \alpha_R^{(0)} [\Delta\Phi_{NS}]^{(0)} \{\Psi_\mu\}^{(0)} \qquad (3)$$

where $[\Delta\Phi_{NS}]$ is the difference matrix of associated modal eigenvector terms.

The describing functions are now employed to compute a set of stiffness values corresponding to these displacements:

$$\{k_{NS}\}^{(0)} = \{f(\delta^{(0)})\} \tag{4}$$

With knowledge of the initial stiffness value of the ith nonlinear spring, a delta or incremental stiffness matrix is generated similar to the stiffness matrix of a simple axial element:

$$[\Delta k_{NS}]^{(0)} = (k_{NS}^{(0)} - k_{NS}^{(I)}) \begin{bmatrix} 1 & -1 \\ -1 & 1 \end{bmatrix} \tag{5}$$

Following similar calculations for each nonlinear spring, a generalized ΔK matrix is formed:

$$[\Delta K]^{(0)} = [\Phi_{NS}]^{(0)T}[\Delta k_{NS}]^{(0)}[\Phi_{NS}]^{(0)} \tag{6}$$

We are now prepared to shift the frequencies and mode shapes of the unmodified system. In accordance with the structural dynamics modification (SDM) method presented by Weissenburger[19] in 1968, the normal mode equations of the dynamic system are recast in the form

$$\left[[M]^{(0)} - \gamma([K]^{(0)} + [\Delta K]^{(0)}) \right] \{\xi\} = 0 \tag{7}$$

where γ is the eigenvalue of the free vibration equation and $\{\xi\}$ is the column matrix of normal mode coordinates. The complete solution of these equations yields n new natural frequencies designated as $[\omega]^{(1)}$. The corresponding mode shapes are computed from

$$[\Phi]^{(1)} = [\Phi]^{(0)}[\Xi] \tag{8}$$

where $[\Xi]$ is the complete set of normal mode coordinates, i.e.,

$$[\Xi] = [\xi_1, \xi_2, \ldots \xi_n] \tag{9}$$

Recalculation of the generalized dynamic properties of the system using the modified frequencies and mode shapes initiates the second step of the iteration. The flutter equations are solved again and the procedure continues until convergence is obtained on the sth iteration. This occurs when the following conditions are met simultaneously:

$$\left| \frac{\delta_i^{(S)} - \delta_i^{(S-1)}}{\delta_i^{(S)}} \right| \le \epsilon \qquad (i = 1, 2, 3, \ldots NSP) \tag{10}$$

where NSP is the number of nonlinearities in the system and ϵ a preselected residual. Once the system has converged, the stability characteristics and flutter mode shape are computed from the eigenvalue and eigenvector of the flutter equation. By varying the reference amplitude d_R, stability curves can be generated as a function of this amplitude. The characteristics of a limit cycle flutter are thus determined or the intitial disturbance required to induce flutter is known.

A factor, referred to as the convergence accelerator, may be applied to the stiffness values of Eq. (4) during subsequent iterations to improve the convergence rate of the scheme. If the nonlinear spring is found to be monotonically converging to the aligned stiffness value, an accelerator greater than one will improve the convergence rate for that spring. If the iterations in stiffness are oscillatory about the aligned value, a convergence accelerator less than one is appropriate. The actual values chosen are at the discretion of the analyst. However, the final solution is independent of the accelerators used.

Describing Functions

An important part of the iterative procedure is the linearization of the dynamic system through the application of describing functions. A thorough review of the basic describing function method as applied to concentrated structural nonlinearities has been presented by Laurenson and Trn.[7] For the purposes of this study, the describing function approach was applied to several generic classes of nonlinearities, with the emphasis on quantifying the accuracy of the resulting functions. To do so, their dynamic behavior in a free-vibration single-degree-of-freedom (sdof) spring-mass system was studied. For some of the simpler nonlinear elements, such as the bilinear spring, closed-form exact solutions exist for their periods and, hence, frequencies. In these cases, a comparison of the results from their describing functions to the exact solutions provides a good indication of the usefulness of the overall describing function approach to linearization. The advantage of the method becomes clearly evident when characterization is required of complicated nonlinearities for which exact solutions do not exist. These can generally be handled with modest computational effort following the describing function approach. The accuracy of these functions is determined by comparison to time domain simulations of the differential equations.

Bilinear Force-Displacement Relationship

A spring with bilinear characteristics is shown in Fig. 2. This type of nonlinearity can possess both softening and hardening properties as illustrated or can become a freeplay nonlinearity with k_1 equal to zero. From the definition of the describing function as the ratio of the equivalent stiffness to a reference spring stiffness, the following relationship can be derived:

$$\Gamma = k_1/k_2 \quad (A < s)$$

$$= \frac{k_e}{k_2} = 1 - \left(1 - \frac{k_1}{k_2}\right)\left(\frac{2t_1}{\pi} + \frac{\sin 2t_1}{\pi}\right) \quad (s \le A < \infty) \tag{11}$$

where A is the oscillatory amplitude and $t_1 = \sin^{-1}(s/A)$. This function is illustrated in Fig. 3 for various values of k_1/k_2. As the amplitude ratio increases, k_2 predominates in both the hardening and softening cases and the describing function value approaches unity. Below an amplitude ratio of 1.0, the system becomes linear and the describing function is constant. An exact closed-form solution for the natural frequency of a spring-mass system with bilinear stiffness
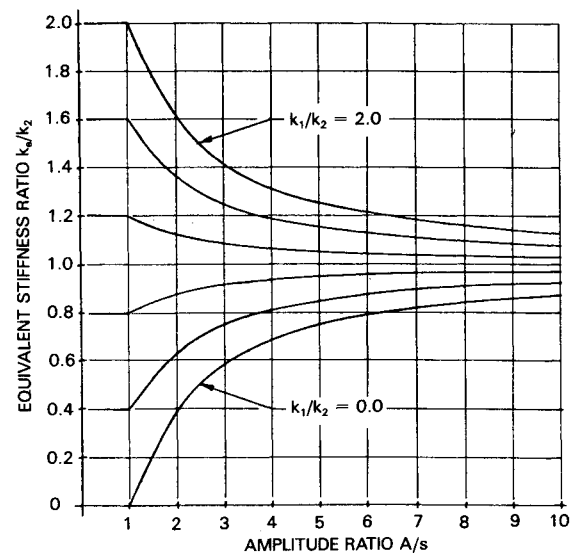

Fig. 3 Bilinear spring describing functions.

characteristics has been developed by Timoshenko and Young.[20] The percent error in the describing function prediction of frequency when compared with the exact solution is presented in Fig. 4. The error becomes large only for very low stiffness ratios and only when the displacement amplitude exceeds the value of s slightly. Even in the worst case when k_1/k_2 is zero, the error is less than 10% for amplitude ratios less than 0.75. The maximum error is quickly reduced as the stiffness ratio increases and is less than 3% for k_1/k_2 of 0.10.

Nonlinear Spring with Freeplay and Hysteresis

The force-displacement relationship for a nonlinear spring with freeplay and hysteresis is illustrated in Fig. 5a. The force developed in the spring (Fig. 5b) is an exponential function of displacement for both increasing and decreasing load paths. The amount of hysteresis is controlled by selection of the powers n and m. The greater the difference $(n-m)$, the greater the hysteresis. The describing function for this nonlinearity can be expressed in terms of the stiffness $k_2 = F_2/s_2$,

$$\Gamma = 0 \quad (A \leq s_1)$$

$$= k_e/k_2 \quad (s_1 < A \leq s_1 + s_2) \tag{12}$$

The equivalent stiffness k_e is

$$k_e = (a_1^2 + b_1^2)^{1/2}/A \quad (s_1 < A \leq s_1 + s_2) \tag{13}$$

where

$$a_1 = \frac{2}{\pi A} \left(\frac{F_2}{s_2^n}\right) (A - s_1)^{n+1} \left[\frac{1}{n+1} - \frac{1}{m+1}\right] \tag{14}$$

$$b_1 = \frac{2}{\pi A} \left(\frac{F_2}{s_2^n}\right) [I_{n+1} + s_1 I_n + (A - s_1)^{n-m} (I_{m+1} + s_1 I_m)] \tag{15}$$

In the expression for b_1,

$$I_n = \int_0^{A-s_1} \frac{z^n dz}{(-z^2 - 2s_1 z - s_1^2 + A^2)^{1/2}} \tag{16}$$

with $z = A\sin t - s_1$. This describing function is illustrated in Fig. 6 for several values of n and m with $s_1 = 0$. In the absence of freeplay, the shape of the force-time history, normalized to the peak force, is identical for any amplitude (i.e., the curves are similar for a given set of n and m values). As a result, the error in the describing function prediction of frequency was found to be constant over the amplitude range. These errors are presented in Table 1 and indicate generally excellent agreement with the numerical results. In all cases, the predictions overestimated the frequency. The general trend is that the error increases with increasing n and m values and with increasing $(n-m)$ values. Over the practical range of these quantities, however, the error remains below 8%. With free play present, the force-time histories are no longer similar and the error increases dramatically for amplitudes just exceeding the free-play region, as was the case with the bilinear spring. The general trends are still evident, but the errors are now a function of amplitude.

To complete the characterization of this nonlinearity, the hysteresis is formulated in terms of an equivalent viscous

Fig. 4 Error in bilinear spring describing function.

Table 1 Error in the describing function prediction of frequency with $s_1 = 0$

n	m	Error, %	n	m	Error, %
1	1	0.0	2	3	4.4
1	2	1.0	2	4	7.8
1	3	2.6	3	3	2.2
1	4	4.9	3	4	6.2
2	2	0.7	4	4	4.0

(a) NONLINEAR FORCE DISPLACEMENT RELATIONSHIP

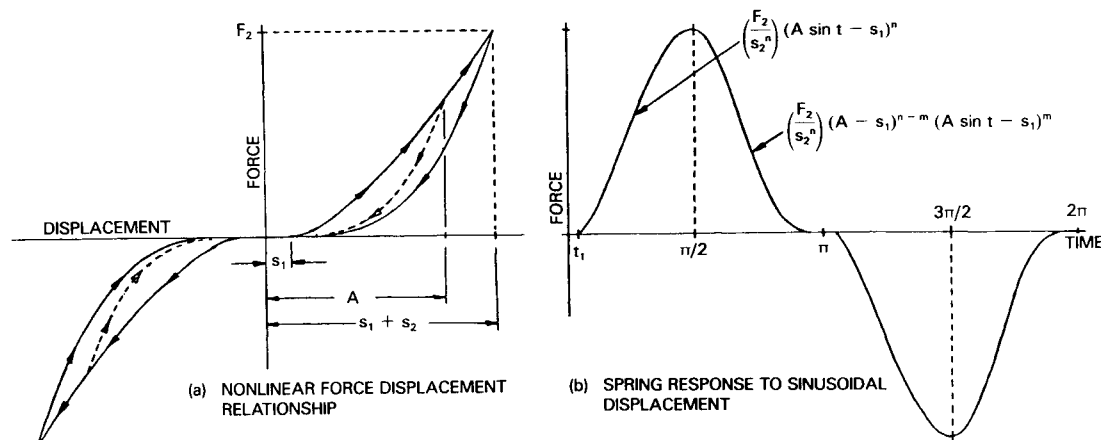(b) SPRING RESPONSE TO SINUSOIDAL DISPLACEMENT

Fig. 5 Nonlinearity with freeplay and hysteresis.

damping ratio. This is accomplished by equating the work done on the nonlinear spring through one cycle of forced motion at its resonant frequency to the energy dissipated by a viscous damping force during a cycle of motion at the same frequency and amplitude. The equivalent viscous damping ratio then becomes

$$\xi_e = a_1/2\sqrt{a_1^2 + b_1^2} \qquad (17)$$

Table 2 gives the results for cases without freeplay in which the damping ratio is constant over the amplitude range. Computed logarithmic decrements from the numerical time histories were used to determine the error in the describing function prediction. Fair to good agreement is achieved with the maximum error at 25.4%. The damping ratio is not consistently overestimated or underestimated nor are there consistent trends in the data.

Validation of the Iterative Procedure

Four examples, ranging from relatively simple configurations to a complex dynamic system with multiple nonlinearities, serve as validation of the iterative method.

Ten Degree-of-Freedom Spring-Mass System

To illustrate the amplitude-stiffness alignment process within the procedure, the 10 dof spring-mass system of Fig. 7 was analyzed. A single free-play nonlinearity was assumed to be present between nodes 1 and 2. The system was excited by a sinusoidally varying displacement with a peak amplitude of 0.254 cm (0.10 in.) applied at node 11. The iterative pro-

cess leading to the proper nonlinear stiffness value is presented in Fig. 8 for an excitation frequency that tracks the first or lowest mode of the system. The iteration begins in the upper left corner of Fig. 8 where, through normal mode summation, the amplitude of the nonlinear spring is determined to be 0.0378 cm (0.0149 in.) for the initial stiffness value of 175 kN/m (1,000 lb/in.). At this amplitude, the describing function prediction of stiffness is zero. A shift in system mode shapes and frequencies using zero stiffness results in a rigid-body mode and a new nonlinear spring amplitude of 0.254 cm (0.10 in.), the same as the excitation amplitude. At this displacement, the nonlinear stiffness is computed to be 135.5 kN/m (744 lb/in.). Applying a convergence accelerator of 0.75 to this value produces a new stiffness estimate for the next iteration of 97.7 kN/m (588 lb/in.). The corresponding amplitude becomes 0.0622 cm (0.0245 in.). The iteration continues in similar fashion until a present convergence criterion has been met. The final values of nonlinear spring stiffness and amplitude are 56.9 kN/m (325 lb/in.) and 0.0937 cm (0.0369 in.), respectively, with the aligned fundamental frequency at 2.00 Hz down from an initial frequency of 2.38 Hz.

The "tuned" system frequencies and mode shapes and thus the final nonlinear spring characteristics are independent of the initial system dynamics, provided that a complete set of modes is used in the iteration. For relatively small dynamic systems, this approach is feasible. However, for larger systems, a truncated series of normal modes is necessary to hold computing costs to an acceptable level. The ability of the structural dynamics modification process to shift mode shapes and frequencies with only a partial set of system dynamics available becomes an important consideration. Table 3 presents the alignment point characteristics for
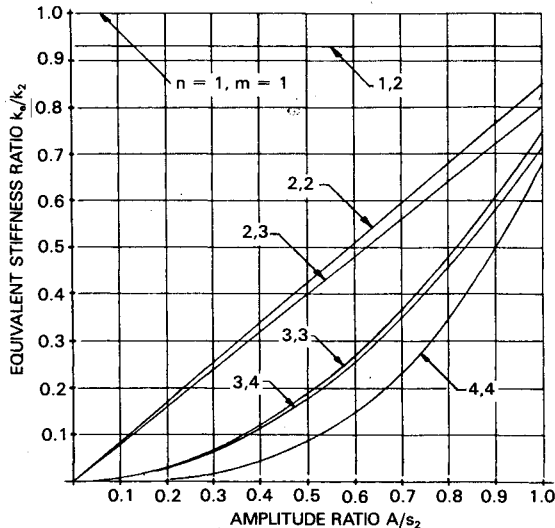

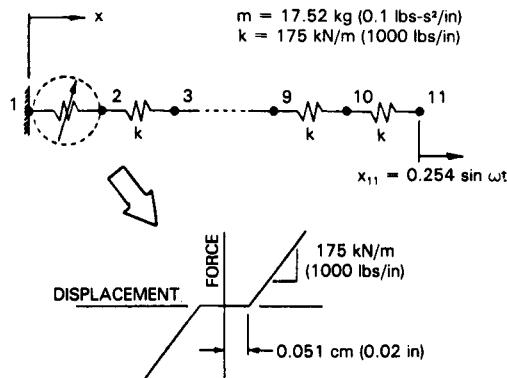Fig. 6 Nonlinear spring describing function with $s_1 = 0$.
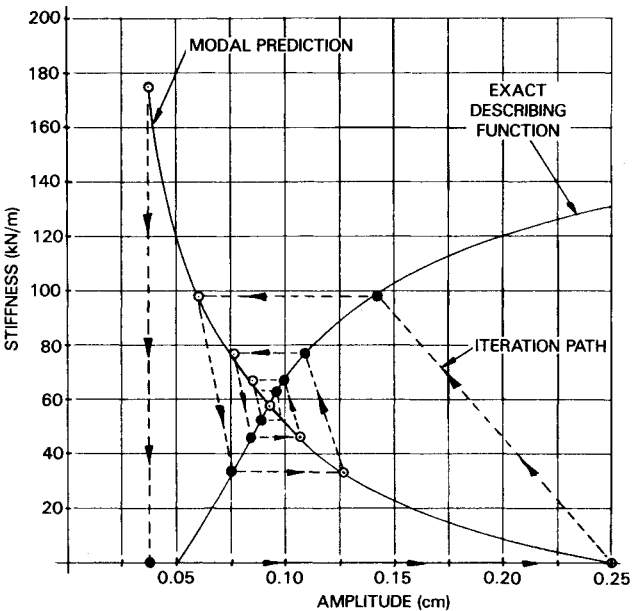

Fig. 7 Ten dof spring-mass system.

Fig. 8 Nonlinear spring amplitude-stiffness alignment process for 10 dof system.

Table 2 Error in the describing function prediction of viscous damping ratio with $s_1 = 0$

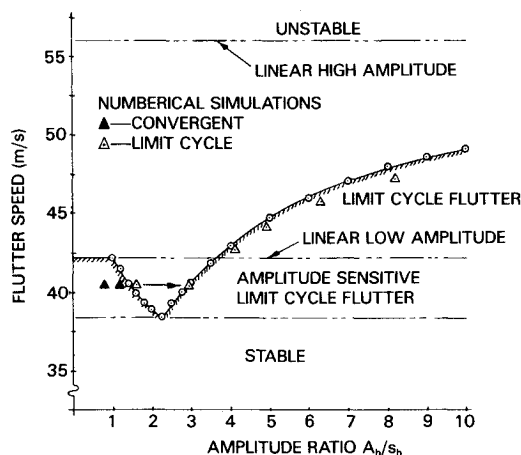| n	m	ξ	ξ_e	Error, %
1	2	0.06453	0.05702	−11.6
1	3	0.11032	0.08948	−18.9
1	4	0.14583	0.11091	−23.9
2	3	0.03049	0.03311	+8.6
2	4	0.05419	0.05522	+1.9
3	4	0.01774	0.02225	+25.4

Table 3   Changes to nonlinear spring alignment point with reduction in the number of modes used in the analysis ($k_e = 175$ kN/m)

Number of modes	Aligned nonlinear spring characteristics	
	Amplitude, cm	Stiffness, kN/m
10	0.0937	56.9
9	0.0932	56.4
7	0.0897	52.2
5	0.0792	38.5
3	0.0610	9.8

Table 4   Changes to nonlinear spring alignment point with reduction in the number of modes used in the analysis ($k_e = 0$)

Number of modes	Aligned nonlinear spring characteristics	
	Amplitude, cm	Stiffness, kN/m
10	0.0935	56.7
9	0.0937	56.9
7	0.0937	57.1
5	0.0942	57.6
3	0.0960	59.5

Fig. 10   Twin control surfaces in supersonic flow.

Fig. 9   Nonlinear flutter boundary for 2 dof flutter model with nonlinearities in both plunge and pitch.

the 10 dof system using successively fewer modes in the iteration. The initial system dynamics in this case were determined with a nonlinear spring stiffness of 175 kN/m (1,000 lb/in.). Although the frequency predictions experience almost no degradation, the predicted nonlinear spring alignment point for the first mode tracking exhibits an unacceptable movement as the number of modes is reduced. The corresponding information for the case in which the initial dynamics include a rigid-body mode are presented in Table 4. Now, the nonlinear spring alignment point holds position very well, with the amplitude and stiffness values being only 2.7 and 4.9% overpredicted with as few as three modes being included in the iteration. Although not conclusive, this example indicates that excellent alignment point predictions can be achieved with relatively few modes if the proper initial system dynamics are used.

Two Degree-of-Freedom Flutter Model

The second configuration analyzed was the "typical section" flutter model experimentally tested by McIntosh et al.[9]
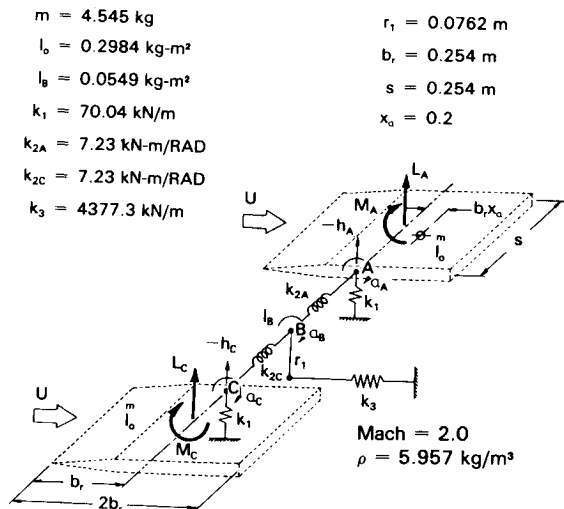
in 1980. Although the tests involved a single bilinear spring in either the pitch or plunge dof, nonlinearities in both positions simultaneously were considered analytically as well. The flutter boundary for the case with nonlinearities in both pitch and plunge is shown in Fig. 9. The results from the numerical simulations as well as the iterative frequency domain approach are included. The unsteady aerodynamics in this case were computed using Theodorsen's[15] equations. At low amplitude ratios, the system acts exactly as it would with only a hardening plunge nonlinearity exhibiting a drop in flutter speed as the plunge amplitude increases. This type of behavior is indicative of an amplitude-sensitive instability in which an initial disturbance of prescribed amplitude is necessary to produce an unstable system. At an amplitude ratio of approximately 2.25, a distinct change occurs with the boundary, reversing its downward movement. The flutter speed continues to increase thereafter and approaches the linear high-amplitude boundary calculated to be 56.1 m/s (184 ft/s). The abrupt change in the boundary can be explained by examining the amplitude ratio of the pitch nonlinearity at the alignment points along the boundary as determined by the iterative procedure. Shown in Table 5, the pitch amplitude ratios remain below 1.0 for plunge ratios up to 2.25. At that point, the pitch ratio exceeds unity and the beneficial effect of increasing the pitch stiffness is immediately evident. Unlike the single nonlinear spring cases, four stability regions exist for this configuration. Unconditionally stable behavior is present at speeds below 38.4 m/s (126 ft/s). Between that level and 42.1 m/s (138 ft/s), an amplitude-sensitive region of stable limit-cycle flutter exists. To illustrate this, consider a speed of 39.6 m/s (130 ft/s). An initial disturbance ratio of less than 1.7 will allow the system to remain stable. Exceeding this value will cause a limit-cycle flutter to occur with an amplitude ratio of about 2.7. Proceeding beyond 42.1 m/s (138 ft/s), a limit-cycle flutter will occur at the amplitude ratios indicated, regardless of the magnitude of the initial disturbance. This third stability region exists up to 56.1 m/s (184 ft/s). Above that speed is the region of divergent flutter.

This example demonstates that the stability boundary of a system with multiple nonlinearities does not necessarily fall between the high- and low-amplitude boundaries predicted by a linear flutter analysis. Knowledge of the amplitude at each nonlinear spring is needed to properly predict the stability characteristics.

Twin Control Surfaces in Supersonic Flow

A more complex dynamic system consisting of the twin control surfaces shown in Fig. 10 was considered next. Using

Table 5 Amplitude-stiffness characteristics at alignment points
along the flutter boundary of 2 dof flutter model

Plunge		Pitch		
Amplitude ratio A_h/s_h	Nonlinear stiffness k_h, kN/m	Amplitude ratio A_α/s_α	Nonlinear stiffness k_α, kN·m/rad	Phase angle Θ, deg
1.00	21.89	0.31	0.0877	−22.0
1.40	24.50	0.50	0.0877	−24.6
2.00	26.58	0.87	0.0877	−28.6
2.25	27.33	1.04	0.0882	−30.1
3.00	28.91	1.30	0.0951	−28.5
4.00	30.15	1.61	0.1029	−26.9
5.00	30.90	1.90	0.1086	−25.7
8.00	32.04	2.73	0.1194	−23.8
10.00	32.43	3.29	0.1238	−23.1
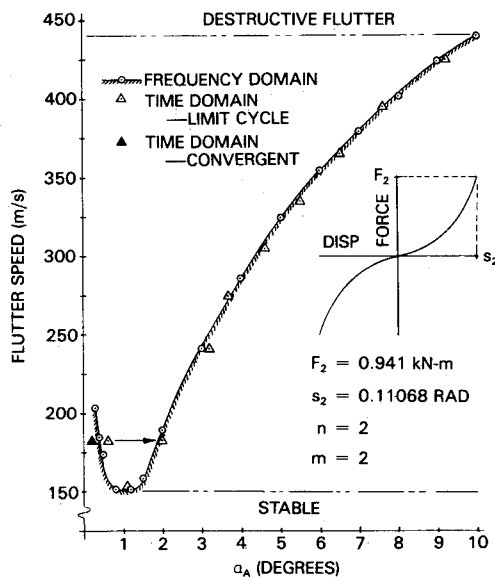
Fig. 11 Flutter boundary for twin control surfaces with nonlinear k_{2A} and k_{2C}.

Fig. 12 Limit cycle oscillations of twin control surfaces with asymmetric initial pluck of $\alpha_A = 2.2$ deg.

piston theory aerodynamics, up to three nonlinearities were analyzed simultaneously with the resulting flutter boundary for the case with two shown in Fig. 11. Identical nonlinearities with parabolic force-displacement relationships were considered to be present in both the k_{2A} and k_{2C} springs. The stability boundary resembles that of the two dof flutter model to some degree and includes the four stability regions discussed. Between $\alpha_A = 1$ and 10 deg, the flutter mode is a symmetric coupling of the first and third normal modes. However, below $\alpha_A = 1$ deg, the flutter mode shape becomes highly asymmetric with control surface C being virtually uncoupled from the system. The pitch displacement α_C is several orders of magnitude below α_A and resembles a "sympathetic" response. Also, it is now 180 deg out of phase with α_A. This region is one of amplitude-sensitive instability and its existence was confirmed with numerical simulations. At 182.9 m/s (600 ft/s), the initial pluck necessary to cause a limit cycle flutter is around 0.4 deg. Below this value, the system remains stable as illustrated by the solid triangle in Fig. 11. Initial disturbances above this amplitude shift the system into a stable limit-cycle flutter with both α_A and α_C oscillating in phase at an amplitude of 2 deg.

The type of initial disturbance necessary to produce flutter is of interest in this region, although the final flutter mode shape remains the same. If the initial pluck is asymmetric (i.e., $\alpha_A = 2.2$ deg, $\alpha_C = 0$), the system will oscillate in the
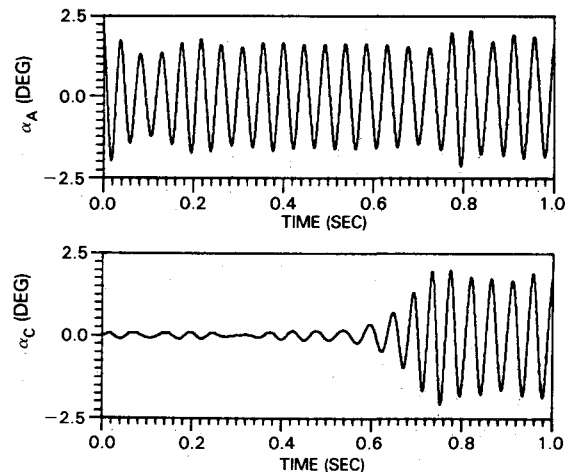
asymmetric mode for a relatively long time with the amplitude α_C gradually building. This is shown in Fig. 12 where more than 0.5 s elapses before the final limit cycle mode shape is acquired. Initially, the oscillation α_C is 180 deg out of phase with α_A, but a gradual phase shift occurs until symmetry is obtained. The closer the initial asymmetric pluck is to 0.4 deg, the longer it takes to acquire the final symmetric mode shape. However, if initial plucks (symmetric or antisymmetric) are imparted to both control surfaces, the phase alignment and acquisition of the final flutter mode shape is much more rapid. It should be noted that the iterative procedure accurately predicts the asymmetric shape as well as the final flutter mode shape.

Tactical Missile Wing Pair

A practical application of the iterative procedure was explored with consideration of the tactical missile wing pair (Fig. 13). This system was relatively large with approximately 700 dof and was analyzed with three nonlinearities of various types. The doublet lattice method and the Mach box method were used to determine the nonlinear flutter boundary in both the subsonic and supersonic flight regimes. In the supersonic case, real-time telemetry data of a limit-cycle flutter (Fig. 14) was used to compare with the amplitude and frequency predictions of the iterative method. Correlation with amplitude was fair, with the telemetry data indictating a peak displacement of approximately 1.2-1.5 deg, while the iterative procedure predicted 0.8 deg using three nonlinearities in the model. The computed flutter mode shape contains some asymmetry with the amplitude of wing 3 greater than
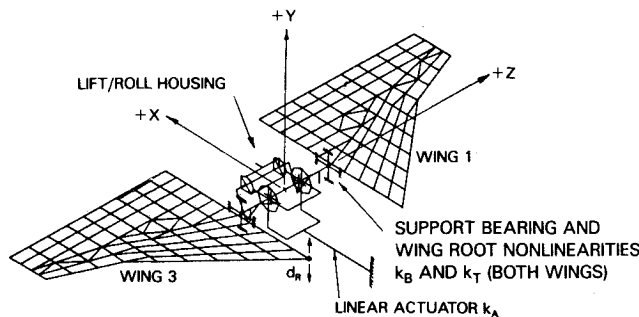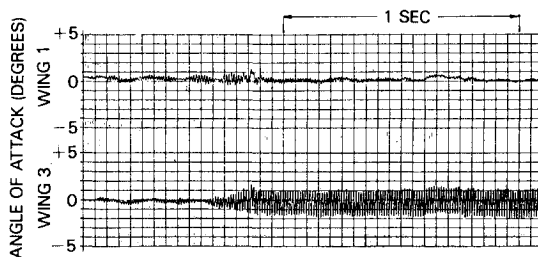
Fig. 13 Tactical missile wing pair.

Fig. 14 Limit cycle flutter of tactical missile wing pair.

wing 1, but not to the extent shown in Fig. 14. The indicated flutter frequency was in the 88-92 Hz range versus a predicted frequency of 96 Hz. It is believed that the inclusion of additional nonlinearities in the analytical model would improve the results.

Conclusions

Conclusions drawn as a result of this study are as follows:

1) As in past studies, the describing function approach to system linearization was found to be a straightforward and reasonably accurate method. When employed in nonlinear flutter analysis, its success is due in large part to the inherent harmonic nature of the phenomenon.

2) The structural dynamics modification procedure has the ability to shift system frequencies and modes shapes when the system is subjected to local stiffness variation. The procedure is exact when all the normal modes of the structure are present. Its accuracy decreases when the number of modes used in the analysis is reduced. However, the error in the technique can be kept to an acceptable level by prudent selection of the initial system dynamics.

3) The iterative procedure is capable of rigorous analysis of large dynamic systems with multiple nonlinearities. The procedure accurately predicts the amplitude of a limit-cycle flutter as well as the magnitude of the initial disturbance necessary to induce flutter. Also, flutter frequencies and complex mode shapes are in agreement with both numerical simulations and experimental data.

4) The computational expense of the iterative procedure is commensurate with the size of the dynamic system. In most cases, however, the expense is minimal. For the examples presented, usually less than 10 iterations were needed at each

point on the boundary to produce an aligned system. The complete boundary of Fig. 11 was determined in less than 1 min of CPU time. In contrast to this, each iteration for the tactical missile wing pair required 3 s of computing time, resulting in a total time in excess of 6 min. The calculations were made on an IBM 3033.

References

[1]Woolston, D. S., Runyan, H. L., and Andrews, R. E., "Some Effects of System Nonlinearities in the Problem of Aircraft Flutter," NACA TN 3539, Oct. 1955.

[2]Woolston, D. S., Runyan, H. W., and Andrews, R. E., "An Investigation of Effects of Certain Types of Structural Nonlinearities on Wing and Control Surface Flutter," Journal of the Aeronautical Sciences, Vol. 24, Jan. 1957, pp. 57-63.

[3]Shen, S. F., "An Approximate Analysis of Nonlinear Flutter Problems," Journal of the Aerospace Sciences, Vol. 28, Jan. 1959, pp. 25-32, 45.

[4]Breitbach, E., "Aircraft Flutter Simulation by Means of the Electronic Analogue Computer with Special Regard to Structural Nonlinearities," ESRO TI-121, Dec. 1974.

[5]Breitbach, E.,, "Effects of Structural Nonlinearities on Aircraft Vibration and Flutter," AGARD-R-665, Jan. 1978.

[6]Breitbach, E. J., "Flutter Analysis of an Airplane with Multiple Structural Nonlinearities in the Control System," NASA TP-1620, Jan. 1980.

[7]Laurenson, R. M. and Trn, R. M., "Flutter of Control Surfaces with Structural Nonlinearities," McDonnell Douglas Astronautics Co., St. Louis, MO, Rept. MDC E1734, Aug. 1977.

[8]Laurenson, R. M., and Trn, R. M., "Flutter Analysis of Missile Control Surfaces Containing Structural Nonlinearities," AIAA Journal, Vol. 18, Oct. 1980, pp. 1245-1251.

[9]McIntosh, S. C. Jr., Reed, R. E. Jr., and Rodden, W. P., "Experimental and Theoretical Study of Nonlinear Flutter," Journal of Aircraft, Vol. 18, Dec. 1981, pp. 1057-1063.

[10]Shen, S. F. and Hsu, C. C., "Analytical Results of Certain Nonlinear Flutter Problems," Journal of the Aeronautical Sciences, Vol. 25, Feb. 1958, pp. 136-137.

[11]Woolston, D. S. and Andrews, R. E., "Remarks on Analytical Results of Certain Nonlinear Flutter Problems," Journal of the Aerospace Sciences, Vol. 28, Jan. 1959, pp. 51-52.

[12]Shen, S. F., "Author's Reply" (to Ref. 11), Journal of the Aerospace Sciences, Vol. 28, Jan. 1959, p. 52.

[13]Theodorsen, T., "General Theory of Aerodynamic Instability and the Mechanism of Flutter," NACA Rept. 496, 1935.

[14]Wagner, H., "Uber die Entstehung des Dynamischen Auftriebs von Tragflugeln (The Occurrence of Aerofoil Dynamic Lift)," ZAMM, Vol. 5, No. 1, Feb. 1925.

[15]Küssner, H. G., "Zusammenfassender Bericht uber den instationaren Auftrieb von Flugeln," Luftfahrtforsch, Bd. 13, Nr. 12, Dec. 1936.

[16]Kryloff, N. and Bogoliuboff, N., Introduction to Nonlinear Mechanics (a free translation by S. Lefschetz), Princeton University Press, Princeton, NJ, 1947.

[17]Dunato, V. W. and Huhn, C. R., "Supersonic Unsteady Aerodynamics for Wings with Trailing Edge Control Surfaces and Folded Tips," AFFDL-TR-68-30, Aug. 1968.

[18]Albano, E. and Rodden, W. P., "A Doublet Lattice Method for Calculating Lift Distributions on Oscillating Surfaces in Subsonic Flows," AIAA Journal, Vol. 7, Nov. 1969, p. 2192.

[19]Weissenberger, J. T., "Effect of Local Modifications on the Vibration Characteristics of Linear Systems," Journal of Applied Mechanics, Vol. 35, June 1968, pp. 327-332.

[20]Timoshenko, S. and Young, D. H., Vibration Problems in Engineering (3rd ed.), Van Nostrand Reinhold Co., New York, 1954.

[21]Lee, C. L., "Aeroelastic Stability Analysis With Interacting Structural Nonlinearities," Ph.D. Dissertation, Southern Methodist University, Dallas, TX, May 1984.